

1 **Investigation of High-Density Polyethylene Pyrolyzed Wax for Asphalt**
2 **Binder Modification: Mechanism, Thermal Properties, and Ageing**
3 **Performance**

4 Charlotte Abdy ^a, Yuqing Zhang ^{b*}, Jiawei Wang ^{c*}, Yi Cheng ^c, Ignacio
5 Artamendi ^d, and Bob Allen ^d

6
7 ^a Department of Civil Engineering, Aston University, Aston Triangle, Birmingham, B4 7ET,
8 UK.

9 ^b School of Transportation, Southeast University, 2 Southeast University Road, Jiangning,
10 Nanjing, 211189, China

11 ^c Department of Chemical Engineering and Applied Chemistry, Aston University, Aston
12 Triangle, Birmingham, B4 7ET, UK.

13 ^d Research & Development and Technical Services, Aggregate Industries UK Ltd.,
14 Derbyshire, DE6 3ET, UK.

15
16 * Corresponding authors, Dr Yuqing Zhang, y.zhang10@aston.ac.uk, Dr Jiawei Wang, +44
17 121 204 3634, j.wang23@aston.ac.uk

18
19 **Highlights**

- 20
21 • Thermal cracking of high-density polyethylene wax in a fixed bed reactor.
22 • Thermal ageing mechanisms in pyrolysis waxes for asphalt modification suitability.
23 • Loss of volatiles, oxidation, and polymerization ageing reactions in pyrolysis waxes.
24 • Optimal pyrolysis wax properties and blending for asphalt binder modification.

25
26 **Abstract**

27
28 The thermal pyrolysis of high-density polyethylene in a fixed bed reactor has been studied in
29 the temperature range of 450-550 °C with two different nitrogen carrier gas flowrates, 2 and
30 4 L min⁻¹, to study the effect of these process parameters as well as the resultant vapour
31 residence times on the formation of wax and its chemical and thermal properties. The
32 technology had a high selectivity to waxes, with a yield of up to 91.87% wax from high-
33 density polyethylene at 500 °C using a nitrogen carrier gas flowrate of 4 L min⁻¹ and
34 subsequent 1.76 second vapour residence time, calculated using the ideal gas law. The waxes
35 were characterised using techniques including gas-chromatography-mass spectroscopy (GC-
36 MS), Fourier transform infrared spectroscopy (FTIR), thermal gravimetric analysis (TGA)
37 and differential scanning calorimetry (DSC). The process operating temperature especially

38 and its subsequent effect on vapour residence times within the reactor had a considerable
39 impact on both the chemical and thermal properties of the waxes. Higher operating
40 temperatures yielded more olefinic waxes due to the promotion of degradation radical
41 mechanisms such as β -scission. They were observed to have higher melting points and
42 thermal stability. An investigation was conducted to assess the thermal properties and ageing
43 performance of the waxes. Thermal conditioning in an ashing oven at 170 °C for 0-6 hours
44 was conducted with a detailed analysis of GC-MS and FTIR at each stage of thermal
45 exposure to further support thermal characterisation results. The changes in chemical
46 composition were attributed mainly to oxidation and polymerisation ageing reactions and
47 were seen to be more prominent in the more unsaturated waxes produced at higher pyrolysis
48 temperatures. The wax produced at 550 °C was determined the optimal wax for binder
49 modification in hot-mix asphalt pavement design due to lower volatile/mass loss. A lower
50 temperature range was suggested for optimal blending conditions to further reduce loss of
51 volatiles with initial blending and storage.

52

53 **Keywords:** Waxes; plastic pyrolysis; fixed bed reactor; ageing; asphalt; sustainable
54 infrastructure

55

56

57 **1. Introduction**

58

59 High-Density Polyethylene (HDPE) is a polyolefin (PO) plastic that has contributed to the
60 recent enormous rise in ‘single-use’ medical waste, generated from various sources during
61 the COVID-19 pandemic (Dharmaraj et al. 2021). The majority of municipal plastic waste
62 streams now comprise of polyethylene plastics such as this, which are typically treated
63 through conventional methods like landfilling or incineration. However, these methods result
64 in new environmental concerns, e.g., air pollution and dioxin emissions, land pollution and
65 even ocean pollution (Onwudili et al. 2009; Tsai et al. 2009; Jambeck et al. 2015; R. Verma
66 et al. 2016; Abdy et al. 2022). The drawbacks associated with these methods make them
67 unsuitable to the goals for sustainable development and the current pressures on waste plastic
68 management has made the development of more sustainable recycling infrastructure vital.

69

70 Currently, organic additives such as waxes have been broadly utilised as viscosity and
71 workability improvers in asphalt binders of higher viscosity, such as rubberised and polymer
72 modified asphalt. Also within warm mix asphalt (WMA) mixtures to achieve reduced process
73 temperatures (100-140 °C) and thus lessen production energy, cost, and emission intensity
74 (Zaumanis and Haritonovs, 2010; Ling et al. 2019; Sukhija and Saboo, 2021). Fischer-Tropsch
75 (Sasobit) wax is a widely researched commercial wax additive studied in literature that is
76 produced synthetically from syngas (Desidery and Lanotte, 2021). The wax reduces binder
77 viscosity at mixing and compaction temperatures as well as produces stiffer mixtures at service
78 conditions. Improved resistance to permanent deformation and interaction between the
79 modifiers (for example, crumb rubber) and base asphalt has additionally been reported (Fazaeli
80 et al. 2012; Yu et al. 2016; SASOL, 2018). Another lower molecular weight product of the
81 polymerization process is polyethylene wax, which is as well largely studied for similar
82 applications. The waxes have been reported to upgrade the rutting (controversial), fatigue, and
83 temperature cracking resistances, as well as improve the moisture resistance of polymer
84 modified WMA (Edwards, 2008; Kim et al. 2013; Nakhaei et al. 2016).

85

86 Alternatively, using PO plastics and plastic derived products as performance-enhancing
87 materials in asphalt binders has also received focused attention for the possible recycling and
88 reuse of this waste material (Leng et al. 2018; Ling et al. 2019). Grady, (2021) reviewed the
89 potential of waste plastics in asphalt concrete and consider this as a practical and cost effective
90 application with the large volumes of both waste and roads being produced. Additionally,

91 conventional asphalt binders are a by-product of the petroleum refining process with petroleum
92 being a finite and highly impacting resource. A main effort within pavement engineering
93 currently is to move towards “greener” alternatives such as this, aiming to align with
94 sustainable development and circular economy goals (Su et al. 2018; Gaudenzi et al. 2021). PO
95 plastics can be thermochemically treated via processes such as pyrolysis which crack the waste
96 into smaller molecular products. This entails heating the materials from moderate to severe
97 temperatures (<800 °C) in an inert atmosphere, the desired products typically being tars (oils
98 and waxes), gaseous products and solid char (Al-Salem et al. 2009). Aliphatic waxes are the
99 primary product of PO thermal pyrolysis at moderate temperatures (500 °C), with a high
100 content of heavy wax hydrocarbons also obtained in the pyrolytic oil (Arabiourrutia et al. 2012;
101 Quesada et al. 2020). Previous literature review work by the authors details the current scope
102 of pyrolysis PO plastics in asphalt binder and hot mix asphalt (HMA) mixture modification
103 (Abdy et al. 2022). It was particularly noted to demonstrate analogous results to binder
104 modification with raw recycled plastics, in both neat and rubberised binders (reduction in
105 penetration point, increase in binder stiffness, softening point, temperature susceptibility and
106 stripping resistance, enhanced resistance to permanent deformation, etc (Al-Hadidy and Tan,
107 2009a, 2009b; Shang and Wang, 2011).) The use of lower mixing temperatures and times while
108 achieving mixture homogeneity was concluded as a clear advantage in the review work, as
109 these lower molecular weight and density products from pyrolysis can be more easily dissolved
110 in bitumen binders (Abdy et al. 2022).

111

112 However, the product spectrum of polyethylene thermal pyrolysis is especially broad and is
113 characterised by a skewed distribution. Due to the random chain scission mechanisms that
114 occur during the primary cracking of thermal decomposition, the wax products that dominate
115 the liquid yield composition at moderate process temperatures are comprised of a wide
116 distribution of hydrocarbon aliphatic compounds, typically within the C₅-C₄₀ range (Williams
117 and Williams, 1997; Ragaert et al. 2017). This non-selectivity resulting in the generation of
118 volatile components within the product waxes is important to consider when matching them to
119 potential applications, such as within asphalt binder modification. Petroleum asphalt containing
120 alternative materials obtained from depolymerisation processes such as pyrolysis, as reported
121 in the case of bio-binders obtained from biomasses, can potentially exhibit quicker ageing when
122 exposed to fresh air at high temperatures (Yang et al. 2015). The ageing of ‘bio-binders’ has
123 been attributed to polymerization and oxidation reactions, as well as the loss of volatiles;
124 resulting in compositional changes, effecting the overall storage stability of the resultant

125 admixture (Hiltner and Das, 2010). A high loss of volatiles especially indicates high emissions
126 and therefore detailed information on the low molecular weight hydrocarbons should be
127 evaluated with respect to influence on the environment and exposure in potential applications.
128 The loss of modifier material may additionally result in it not fully imparting performance
129 enhancing properties onto the asphalt binder admixture. Therefore, there is much significance
130 in the optimisation of the pyrolysis process in obtaining waxes with optimal compositions for
131 blending and reducing the volatiles present within the subsequent modified asphalt binders.
132 Optimal wax modifiers should be able to exhibit both chemical and thermal stability when
133 subjected to high-speed shear mixing with neat binders; in literature commercial waxes and
134 waxes obtained from thermal degradation processes are typically blended between 115-180 °C
135 for 10-30 minutes (Edwards, 2008; Dimondo and Guillon, 2017; Ling et al. 2019). Also during
136 the thermal conditioning processes for long- and short-term ageing that are conducted on the
137 modified binders; the rolling thin-film oven test (RTFOT) and pressure ageing vessel (PAV),
138 allowing for full binder characterisation with respect to the main pavement failure modes such
139 as fatigue and rutting (BSOL, 2012, 2014). Furthermore, optimisation to obtain a desired
140 product decreases process uncertainty and increase the credibility and economic viability of
141 the process for investment and commercialisation.

142

143 A small portion of studies have used optimised experimental configurations (e.g., vacuum
144 pyrolysis, conical spouted reactor) suitable for the selectivity of obtaining pyrolysis waxes,
145 the primary devolatilization product in polymer degradation in pyrolysis. Through
146 characterisation, the waxes presented as similar to commercial paraffin waxes and suitable
147 for certain fuel and other applications (Aguado et al. 2002; Arabiourrutia et al. 2012). Yet a
148 research gap identified in previous review work was the lack of extensive characterisation of
149 the modifier materials derived from waste and the full determination of their suitability for
150 asphalt binder modification prior to blending and binder analysis (Abdy et al. 2022).

151 Therefore, no fully established relationships have been made between the thermal and
152 chemical characteristics of the pyrolysis waxes from HDPE and the subsequent mechanical
153 and rheological performance of the modified asphalt binders. Furthermore, without such
154 relationships, optimal wax properties have not been identified for this application, leading to
155 a lack of optimisation of the pyrolysis process for desired products.

156 Using a fixed bed reactor to obtain wax from the thermal pyrolysis of HDPE, this paper
157 describes the first phase of a broader work, in which pyrolysis mechanisms and wax yields are

158 described, and relationships between the process operating parameters and resultant wax
159 chemical and thermal properties are established. Its novelty is its focus on the thermal
160 properties and ageing performance of the waxes, especially with regards to volatile loss and
161 the proposed ageing mechanisms that occur. This can be linked to the chemical composition of
162 the wax and thus the pyrolysis parameters utilised that result in certain pyrolysis reaction
163 mechanisms. The techniques utilised to assist in this investigation include non-isothermal
164 thermogravimetric analysis (TGA) and differential scanning calorimetry (DSC) to examine the
165 thermal degradation characteristics and melting point ranges of the unaged waxes. Gas
166 Chromatography-Mass Spectroscopy (GC-MS) and Fourier Transform Infrared Spectroscopy
167 (FTIR) are used to quantitatively determine the chemical composition and distribution as well
168 as qualitatively identify the chemical functional groups present in the pyrolysis waxes,
169 respectively. The two latter techniques especially are used to comprehensively analyse the
170 unaged and thermally aged waxes, in order to propose ageing mechanisms that take place.
171 These techniques in conjunction can be used to assess the ageing performance of the waxes
172 such that optimal waxes can be taken forward in later work for blending with asphalt binders.

173

174

175

176

177

178

179

180

181

182

183

184

185

186

187 **2. Materials and Methods**

188

189 *2.1. Materials*

190

191 High-density polyethylene (HDPE) was sourced from Sigma-Aldrich in the form of
192 approximately 2 x 2 mm² clear round pellets (injection moulding grade). The materials
193 physical properties were declared in the MSDS as density ($\rho = 0.952$ g/mL), melt index (MI;
194 12 g/ 10 min), visca softening point (125 °C), and melting point (125-140 °C).

195

196 *2.2. Thermal Pyrolysis*

197

198 The HDPE pellets were pyrolyzed using a bench scale system at 450-550 °C to examine the
199 influence of operating temperature on product wax yield and properties. As seen in Figure 1,
200 the system consisted of a fixed-bed reactor vessel containing a metal crucible that was first
201 filled with 20 g of metal balls to provide improved heat transfer within the crucible, followed
202 by 25 g of HDPE pellets for every batch pyrolysis reaction. The dimensions of the reactor
203 tube were a 50.8 mm diameter and a 150 mm length. A Carbolite electric furnace model EVT
204 12/150B with a power capacity of 750 watts was used as the external heating source. Prior to
205 each experimental run, the system was purged with nitrogen (N₂) gas to eliminate the
206 presence of oxygen. Upon exiting the pyrolysis reactor, the gases passed through a 5 °C water
207 condenser and further glassware for wax product condensation and collection. A cotton wool
208 filter was in place to capture any escaping vapours and the non-condensable gases were
209 vented. Using this reactor configuration, the HDPE pellets were thermally degraded
210 gradually, achieving the final temperature using a heating rate of 10 °C min⁻¹. Volatile
211 products were purged from the reactor tube using two nitrogen flowrates (2 and 4 L min⁻¹) to
212 additionally observe the influence of vapour residence time on the yield and properties of the
213 pyrolysis wax products. The vapour residence times were estimated using the ideal gas law
214 for the carrier gas and can be found in Table 1. The condensed wax product was collected
215 after >2 hours of pyrolysis reaction time without separating the light and heavy fractions. All
216 experiments were conducted in triplets. The product waxes were named according to the
217 pyrolysis parameters used, for example the pyrolysis wax produced at 450 °C with a 2 L min⁻¹
218 ¹ carrier gas flowrate is referenced to as sample 450-2, and so on.

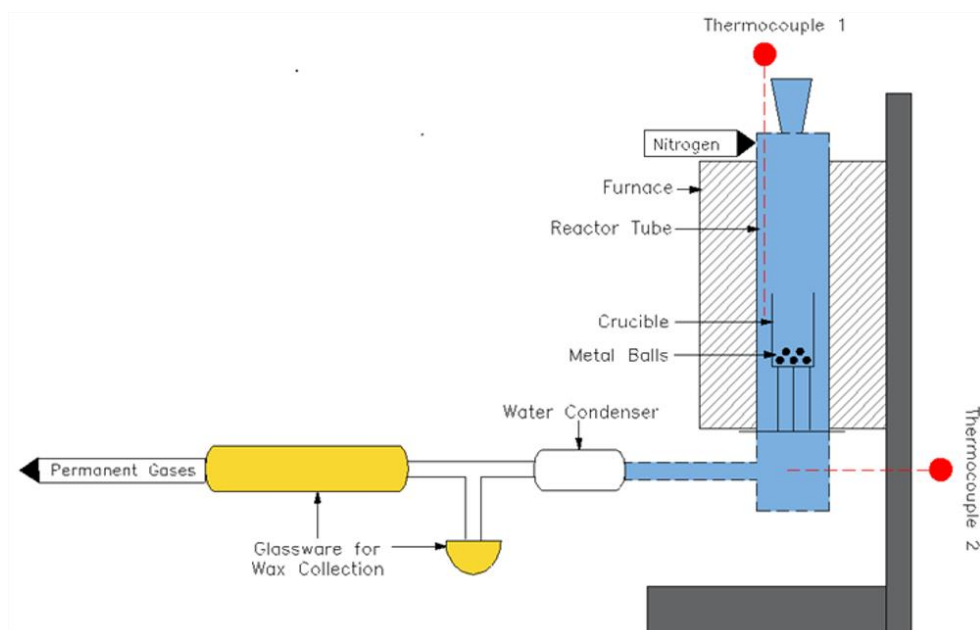
219

220 **Table 1:** Pyrolysis conditions.

Pyrolysis Temperature (°C)	Nitrogen (N ₂) Flowrate (L min ⁻¹)	Vapour Residence Time* (s)
450	2	3.76
	4	1.88
500	2	3.52
	4	1.76
550	2	3.30
	4	1.65

221 *Vapour residence time was estimated using Ideal Gas Law.

222
223



224 **Figure 1.** Schematic diagram of the bench scale pyrolysis reactor system used in this study.

226

227 2.3. Wax Characterisation

228

229 Fourier transform infrared (FTIR) spectroscopy was employed in attenuated total reflectance
230 mode (ATR) for the chemical characterisation of the pyrolysis wax samples. The IR spectra
231 of the waxes obtained were recorded on a PerkinElmer Frontier Spectrometer, with the
232 wavelength range 400-4000 cm⁻¹, 32 scans and a 4 cm⁻¹ resolution. This was as well used to
233 demonstrate the repeatability of the waxes between pyrolysis runs.

234

235 The wax samples were additionally submitted for gas chromatography-mass spectroscopy
236 (GC-MS) chemical analysis. Prior to submission, the waxes were dissolved in toluene and
237 filtered using PTFE 0.2µm filters. A Shimadzu GC-MS-QP2010 SE model was used for the
238 analysis using a GC program of 50 °C to 300 °C with a heating rate of 10 °C/min (Al-Salem

239 et al. 2020). The method proposed by Szulejko et al. (2013) to predict gas chromatographic
240 mass response factors (RF) based on the theory of effective carbon numbers (ECN) was used
241 to interpret the experimental data.

242 Thermogravimetric analysis (TGA) was utilised to examine the thermal characteristics of the
243 pyrolysis wax materials. Additionally, it was applied as an indicator for the thermal stability
244 of the waxes for potential applications such as within asphalt pavements as alternative binder
245 materials at 150-170 °C. A Perkin Elmer Pyris 1 TGA was used to analyse the pyrolysis
246 waxes from 20-600 °C with a heating rate of 10 °C min⁻¹ under a constant flow of pure
247 nitrogen (N₂) gas at 30 mL min⁻¹. Differential Scanning Calorimetry (DSC) was carried out
248 to measure the melting point of the pyrolysis waxes, using a Mettler Toledo DSC 1 from 25-
249 200 °C with a heating rate of 5 °C min⁻¹, done in an inert atmosphere using aluminium
250 containers.

251

252 *2.4 Wax Ageing Experiment*

253

254 To provide further interpretation of the results obtained from both TGA and DSC analyses,
255 an additional experimental setup was arranged for the thermal conditioning of the waxes in an
256 ashing oven set at 150 °C for 0, 1, 3, and 6 hours. From the mass loss, the total loss of
257 volatiles could be determined. The GC-MS and FTIR techniques mentioned previously were
258 utilised to show the effects of somewhat short-term ageing on the wax chemical composition.
259 This was also utilised as an indicator for the suitability of pyrolysis waxes in asphalt
260 pavement production, in which the bitumen binders are heated for prolonged times during
261 mixing and storage. All ageing experiments were repeated three times.

262

263 **3. Results and Discussion**

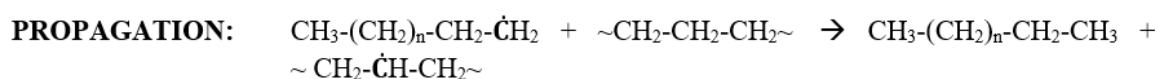
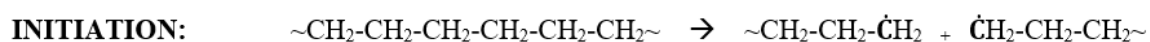
264

265 *3.1. Pyrolysis Yields*

266

267 Polyolefin pyrolysis consists of a set of free-radical reaction mechanisms, predominantly
268 yielding a broad product spectrum of lower molecular paraffins and α -olefins (C₁ to C₅₀). The
269 plastic degradation mechanism has been previously described to involve three main steps that
270 occur sequentially, being initiation, propagation, and termination (Horvat, 1999; Al-Salem et
271 al. 2017). During the initiation reaction, the polymer chain undergoes a random homolytic
272 scission, initiating the mechanism by producing primary radicals. Moreover, hydrogen

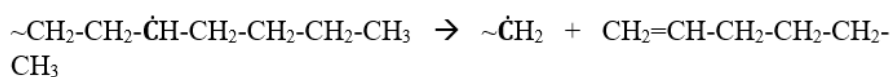
273 abstraction and β -scission are considered as the propagation steps and are associated
 274 particularly with the degradation of PO plastics [39]. Hydrogen abstraction (intermolecular)
 275 entails the transfer of hydrogen between the primary radicals and hydrocarbon chains to
 276 produce new hydrocarbon products as well as more stable radicals. β -scission involves the
 277 scission of paraffin, olefin and diolefin radicals to produce olefin or diolefin products, as well
 278 as a new radical. The thermal degradation is completed by a recombination reaction which
 279 generates a smaller residual polymer chain (Savage, 2000; Mastral et al. 2007). The radical
 280 chain mechanisms can be seen in Figure 2. Typically, waxy materials in the C₂₀-C₅₀ range are
 281 produced in the primary devolatilization reaction of pyrolysis. These primary products are
 282 cracked further in secondary reactions to yield mainly olefinic hydrocarbons. Though, the
 283 gaseous products are highly reactive and thus further tertiary reactions take place to form
 284 more stable compounds, including aromatics. The process may also yield additional products
 285 such as hydrogen, methane and coke when the product stream undergoes a long residence
 286 time (Aguado et al. 2002; Al-Salem and Dutta, 2021).
 287



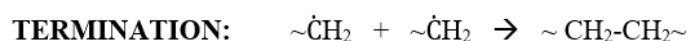
(Hydrogen abstraction, alkane production)



(β -scission of the primary radical)



(β -scission, alkene production)

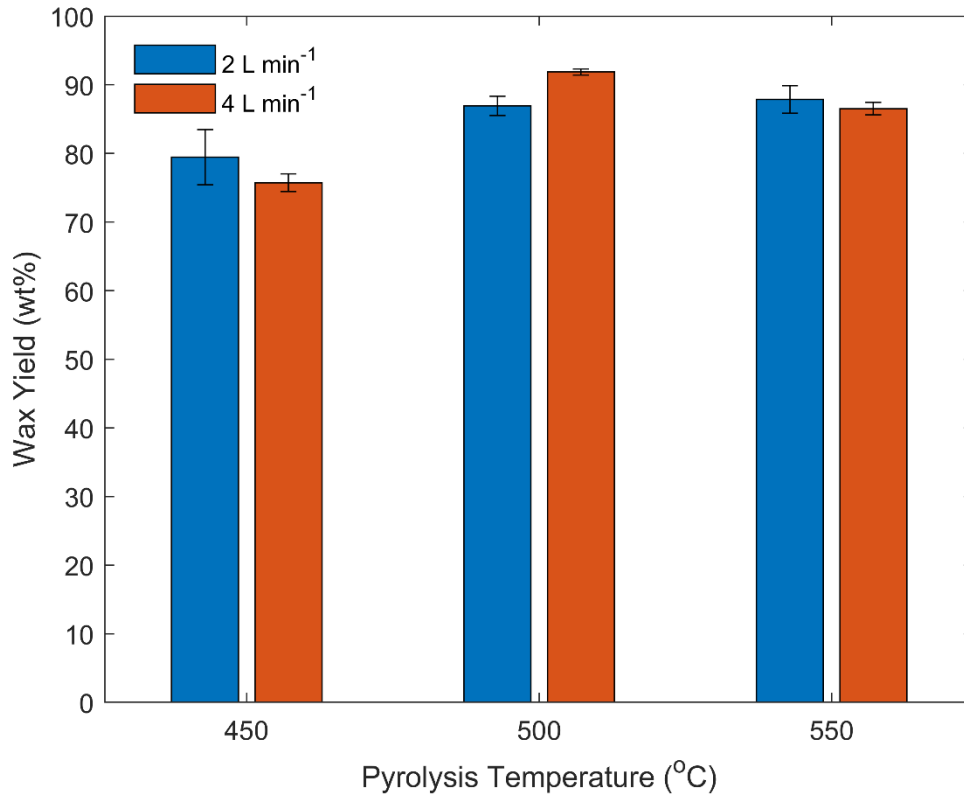


(Recombination)

288
 289 **Figure 2.** Radical mechanism of the thermal degradation of polyethylene, taken from
 290 (Bockhorn et al. 1999; Horvat, 1999).
 291

292 In this study, the two controllable variables were the pyrolysis temperature and carrier gas
293 flowrate. Figure 3 shows the wax yield with respect to the process conditions described in
294 *Section 2.2*. The yield of wax obtained for HDPE pyrolysis is higher than that reported by Al-
295 Salem and Dutta, (2021). in a fixed-bed reactor at 500 °C, which was 32 wt%. Nevertheless,
296 Arabiourrutia et al. (2012) saw a similar yield in a conical spouted bed reactor at 450 °C of
297 80 wt%. A prominent trend reported in literature is the favouring of secondary cracking
298 reactions at high operating temperatures, which generates more gaseous products and in turn
299 reduces the formation of wax products (Williams and Williams, 1999a; Aguado et al. 2002;
300 Arabiourrutia et al. 2012; Al-Salem et al. 2017). This is due to the increased concentration of
301 short radicals from favouring the vaporisation of long chains and as a consequence increasing
302 the rate of this process. In this study, the trend in wax yield with increasing pyrolysis
303 temperature differs to this, such that the wax yield increases with temperature from 75.73-
304 79.46 wt% at 450 °C to 86.53-87.86 wt% at 550 °C. The wax yield is only seen to decrease
305 with temperature from 91.87 wt% at 500 ° to 86.53 wt% at 550 °C at the higher carrier gas
306 flowrate of 4 L min⁻¹. For HDPE, an initial increase in wax yield at increasing low-moderate
307 operating temperatures (500-600 °C), followed by a yield decrease at higher temperatures
308 (600+ °C) was also reported by Al-Salem and Dutta, (2021). This result can be explained as a
309 consequence of the low branched structure of HDPE. For polyolefins with a higher degree of
310 branching (polypropylene), at lower temperatures (450-500 °C), cracking initially takes place
311 in branched chains. At the short residence times achieved by reactor configurations designed
312 for optimised wax production, the cracking of principal chains is low. At temperatures of
313 450-500 °C, the cracking of HDPE feedstock to gases is favoured, which may later be
314 condensed to pyrolysis oils. Furthermore, it was reported that commingled plastic solid waste
315 (PSW) consisting of mildly branched feedstock (such as HDPE) with 10 wt% of the higher
316 branched PP yielded no wax at 500 °C and produced low yields at 600 and 800 °C (Al-Salem
317 and Dutta, 2021). It was attributed to the mildly branched, more crystalline feedstock
318 requiring higher temperatures and residence times (Aguado et al. 2002; Al-Salem and Dutta,
319 2021). This was consistent with their lower wax yield from HDPE pyrolysis at 500°C and
320 agrees with this work at 450-500 °C. Another explanation is that a lower residence time as a
321 result of increasing the temperature in the reactor reduces cracking of the feedstock, therefore
322 higher molecular chain hydrocarbons are obtained (Adrados et al. 2012). One governing
323 factor in the pyrolysis of PO polymers is the residence time of the feedstock material in the
324 reactor; longer residence times increases the cracking of primary products to more thermally
325 stable products, favouring the production of oils (Mastral et al. 2003). Moreover, Park et al.

326 (2002) reported the non-isothermal pyrolysis of low-density polyethylene (LDPE) at 440 °C
327 in a semi-batch reactor, noting that the retention time increased in the low temperature region
328 and a subsequent increase in ratio of lower molecular weight products.



329 **Figure 3.** Yields (wt%) of wax with respect to the reactor operating conditions.
330
331

332 In terms of the effect of the carrier gas flow rate and subsequent vapour residence times
333 calculated at each temperature, a faster nitrogen flowrate decreased the yield of wax at 450
334 °C, which could be attributed to a cooling effect, as the nitrogen was not preheated prior to
335 entering the reactor system and it has been established that due to the structure of HDPE, it
336 may require more elevated temperatures for higher wax yields. The only increase in wax
337 yield with an increase carrier gas rate is at 500 °C, whereas the yields are somewhat similar at
338 each flowrate at 550 °C. It can be comprehended that the effect of the operating temperature
339 and its subsequent vapour residence time had a larger effect on the resultant wax yields. The
340 predominant influence of reactor temperature on the resultant spectrum of pyrolysis products,
341 more so than other process parameters, has been reported by other authors. This is due to the
342 temperature being the key parameter in controlling the cracking mechanisms of the polymer
343 chains (Westerhout et al. 1998; Kumar and Singh, 2011).

344

345 3.2. Wax Chemical Characterisation

346

347 Infrared spectra of the waxes obtained at the pyrolysis parameters studied are shown in
348 Figure 4. The spectra are analogous to each other and it is noted that they are also comparable
349 to those obtained by (Chaala et al. 1997). for commercial paraffinic wax as well as pyrolysis
350 wax obtained from the vacuum pyrolysis of polyethylene based electric cables. There are
351 two bands corresponding to the stretching of $\text{-CH}_2\text{-}$ groups at 2920 and 2850 cm^{-1} , as well as a
352 doublet seen at 725 cm^{-1} which relates to the skeletal vibrations of these C-H groups. Two
353 shoulders are observed at 2960 and 2900 cm^{-1} which correspond to -CH_3 terminal bond
354 groups. Aguado et al. (2002) noted that these are much weaker for pyrolytic waxes than for
355 commercial waxes, inferring that the alkyl chains of waxes obtained from pyrolysis are less
356 branched than those produced commercially. Deformation vibrations of these C-H alkyl
357 groups are additionally observed by the bands at 1465 and 1380 cm^{-1} . When comparing the
358 spectra of this study with those produced by (Chaala et al. 1997). for commercial waxes, it is
359 noticed that the waxes obtained from plastic pyrolysis are more unsaturated, the generation of
360 -C=C- olefinic groups explained by the occurrence of radical degradation mechanisms such
361 as β -scission. The bands located at 3040 , 1645 and in the $890\text{-}995\text{ cm}^{-1}$ range correspond to
362 C-H deformation vibrations of olefinic bonds, stretching of conjugated alkene groups and R-
363 CH=CH_2 , trans -CH=CH- and $\text{R}_1\text{R}_2\text{C=CH}_2$ groups, respectively (Aguado et al. 2002).

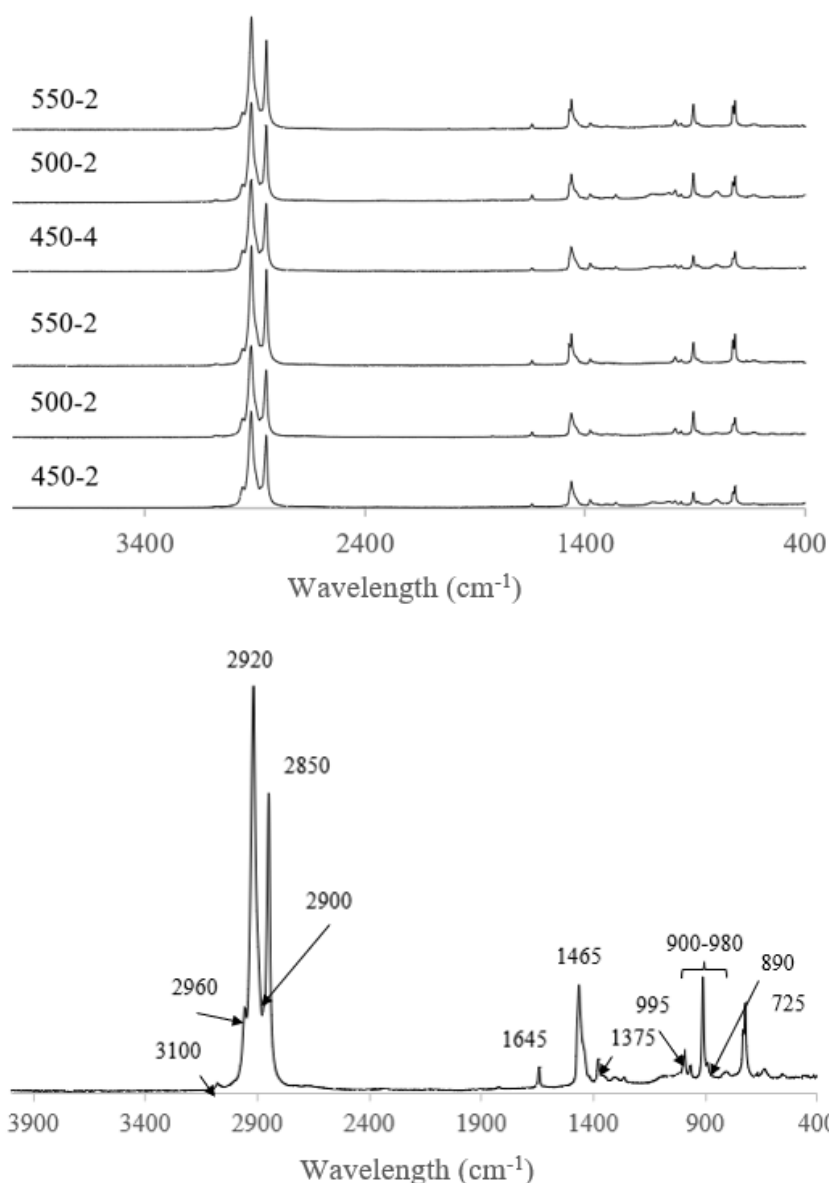


Figure 4. FTIR Spectra for HDPE Pyrolysis Waxes.

364
365
366
367

368 The GC-MS chromatograms produced for the pyrolysis waxes are appended in Figure S1 (a-
369 g) and show homologous series of triplets that are typical of HDPE depolymerisation. (Lund
370 et al. 2008). Within the spectrum, each triplet is comprised of an α,ω -diene, olefin and
371 paraffin for each carbon number (Al-Salem et al. 2020). In addition, trace amounts of
372 branched and cyclic hydrocarbons between the triplets as well as noticeable peaks for
373 aromatic components, such as benzene and xylene, can be seen at the lower retention times
374 within the spectrum. The mass response factors and thus percentiles were calculated for each
375 component and the peak areas were integrated and totalled for representative categories:
376 gasoline range ($<C_{12}$) and high molecular weight (MW) hydrocarbon ($C_{13}<$) components, as

377 well as the class of hydrocarbons (aromatic, paraffinic, olefinic and diene) present in each
 378 sample, as shown in Table 2.

379

380 **Table 2:** Distribution of hydrocarbons in each pyrolysis wax sample and percentile
 381 distribution in gasoline and high MW categories, as well as class of components.

	450-2	500-2	550-2	450-4	500-4	550-4
Gasoline Range (<C ₁₂)	25.87	25.76	26.37	22.92	29.93	30.18
High MW (C ₁₃ >)	74.13	74.24	73.63	77.08	70.07	69.82
Aromatic	3.38	3.48	2.91	2.45	1.83	2.38
Paraffinic	57.53	39.57	36.70	61.83	38.11	35.53
Olefinic	36.03	49.65	51.38	35.72	54.53	54.79
Diene	3.06	7.29	9.00	0.00	5.53	7.30

382

383 The wax samples were extremely viscous (semi-solid) at room temperature, and the majority
 384 of each sample eluted in the higher molecular weight carbon range (C₁₃>). It is observed that
 385 heavy hydrocarbons did not elute with a considerable differentiation from the baseline due to
 386 the GC-MS program utilised, as also observed by Al-Salem et al. (2020). This should be
 387 considered when the heavy components are analysed. However, this program is still
 388 considered as suitable as it meets the criteria previously outlined by Lund et al. (2008) for the
 389 analysis of plastic depolymerisation. Kumar and Singh, (2013) reported the characteristics of
 390 heavy hydrocarbon thermal degradation to include poor gasoline selectivity, with a wide
 391 distribution of light molecular weight products. The results and chromatograms show that this
 392 work is in agreement mainly due to the reactor system operating under thermal (non-
 393 catalytic) pyrolysis conditions, therefore fuel production is not favoured. Furthermore, it can
 394 be seen that the operating temperature has the most significant effect on the cracking and wax
 395 product composition, rather than the effect of the carrier gas flow rate on volatile residence
 396 times in the reactor system.

397 It is generally established that increasing the pyrolysis temperature results in a reduction of
 398 residence time, lowering the cracking reaction rates and thus a generating higher molecular
 399 weight compounds (oils and waxes (Adrados et al. 2012)). Noticeably in this work, with the
 400 increase in pyrolysis temperature, the percentage of gasoline range hydrocarbons is seen to
 401 rise. Specifically, the increased generation of C₆-C₈ aliphatic compounds is noted, such as 1-
 402 hexene, 1-heptene and 1-octene. Similar observations have been made; Hernández et al.
 403 (2007) conducted thermal pyrolysis of HDPE in a fluidised bed reactor. Yields of these
 404 compounds (especially *n*-hexane) were reported to have increased due to the extension of

405 secondary propagation reactions of intermediate compounds, facilitated by high operating
406 temperatures and low residence times.

407

408 Al-Salem, (2019) saw an initial increase in high molecular weight compounds in the product
409 oil with increasing operating temperature (500-600 °C), for the thermal cracking of HDPE in
410 a fixed bed reactor. However, the authors also saw an increase in gasoline range compounds
411 with the further elevation of bed temperatures (600 °C+) as a consequence of further cracking
412 reactions. In this work, the pyrolysis temperature is seen to have a dominating impact in
413 promoting secondary cracking reactions to generate smaller compounds (C₆-C₈) within the
414 gasoline range, that are too promoted (to an extent) at higher temperatures with lower
415 residence times, thus reducing the mass% of C₁₃< wax compounds somewhat. Williams and
416 Williams, (1999b) summarised their analysis of the oil and wax products from the thermal
417 pyrolysis of mixed plastic waste, solely confirming aliphatic products comprising of
418 paraffins, olefins and diolefins. The latter possibly a result of propagation intramolecular
419 hydrogen transference and β-scission mechanisms (as described in Figure 2). Ghasr and
420 Abedini, (2017) produced a mechanistic model to predict the product distribution of HDPE
421 pyrolysis in a conical spouted-bed reactor, based on the radical mechanisms previously
422 discussed. The results showed that the fastest reaction and controlling propagation stage in
423 cracking is β-scission for the production of olefins and dienes. The importance of other stages
424 was also emphasised, such as hydrogen abstraction in the role of paraffin and diene
425 production. The main product was olefin, while the amount of diene production increased
426 significantly with increasing temperature. Other authors have reported similar for the thermal
427 pyrolysis of HDPE (Mastral et al. 2007; Kumar and Singh, 2013). This work is mainly in
428 agreement with the findings of the mechanistic model, with the exception of paraffinic
429 compounds being the main product at the lower pyrolysis temperature of 450 °C, which
430 generated trace-small amounts of diene compounds.

431 Aromatics such as benzene belong to a group of compounds which yield increases by
432 increasing the residence time and temperature (Hernández et al. 2007). Jung et al. (2010)
433 suggested that the Diels-Alder reaction mechanism followed by dehydrogenation may result
434 in aromatic production from the catalytic pyrolysis of polypropylene/polyethylene. Generally,
435 raising the pyrolysis temperature increases the formation of aromatic hydrocarbons as it
436 promotes the rapid release of radicals which undergo intramolecular exchanges to produce
437 cyclic compounds (Seeger and Barrall, 1975; Al-Salem, 2019). Additionally, high residence
438 times and temperatures favour secondary reactions that produce highly reactive gaseous

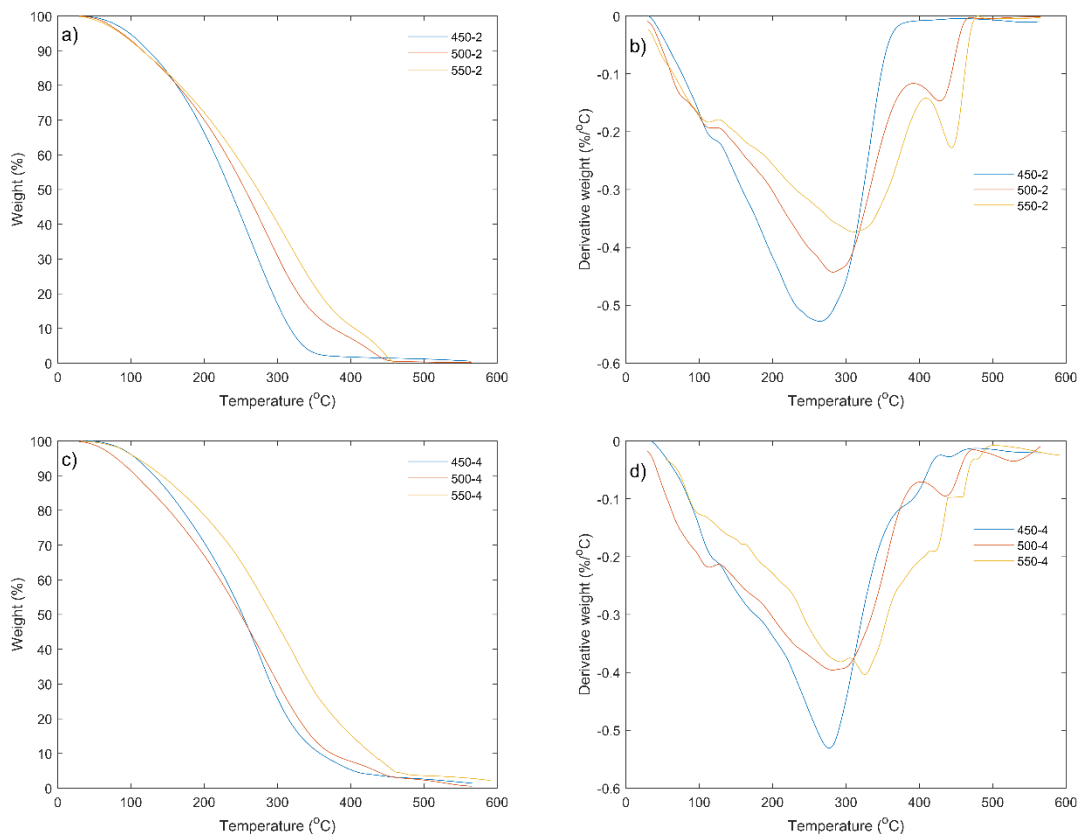
439 products, allowing for tertiary reactions to form more stable aromatics compounds. In this
440 study, small amounts of benzene, ethyl benzene and xylene were seen in the lower region of
441 the chromatograms. The amount of aromatics in the wax samples varies between 1.83-3.48%,
442 the carrier gas flowrate does not largely affect the yield of cyclic compounds present,
443 however, it is observed that the aromatic yield is higher for the reactions with a 2 L/min
444 carrier gas flowrate, corresponding to slightly higher residence times. Overall, a slight
445 decrease in aromatics can be seen as the temperature parameter is increased, suggesting that
446 the effect of temperature on volatile residence times within the reactor has a larger influence
447 on aromatic production in this reactor system.

448

449 *3.2 Wax Thermal Characterisation*

450

451 Representative TGA and DTG thermograms for each pyrolysis wax thermal degradation as a
452 function of pyrolysis conditions (temperature, carrier gas flowrate) are presented in Figure 5.
453 HDPE typically shows a two-stage decomposition process; the initial degradation starts at a
454 lower temperature and propagates gradually until the second degradation stage is reached in
455 which a sharp degradation is observed (Miandad et al. 2019). The pyrolysis of HDPE
456 significantly shortens the initial stage of thermal decomposition in the wax products and the
457 rapid weight loss of hydrocarbons now happens over a wider temperature range, as the
458 pyrolysis has yielded a broad spectrum of small molecular weight hydrocarbons. The
459 maximum degradation of PE is typically achieved within 420-490 °C, whereas this can be
460 seen to happen between 90-460 °C for the pyrolysis waxes. As the temperature was increased
461 for the pyrolysis, an increase in thermal stability, or a decrease in volatility, of the pyrolysis
462 waxes was observed. This infers that heavier hydrocarbon chains are generated and distilled
463 during the chain scission mechanism at higher pyrolysis temperatures. The effect of carrier
464 gas flowrate on vapour residence time is also seen to influence the thermal properties of the
465 waxes, with the waxes produced using a faster nitrogen flowrate having a slightly higher
466 thermal stability, for the same reason as the higher temperature conditions. These results for
467 thermal stability of the waxes indicate their potential suitability in asphalt pavement
468 applications such as alternative binder materials, as these are incorporated into bitumen at
469 temperatures of 150-170 °C.



470

471

472

473

474

Figure 5. Representative TGA and DTG thermograms for the pyrolysis waxes as a function of pyrolysis conditions (temperature, carrier gas flow rate.)

475

476

477

478

479

480

481

482

483

484

485

486

487

488

489

490

Waxes are mixtures of different size and nature molecules and therefore do not have a defined characteristic melting point that pure substances have (Dwivedi, 2017). Therefore, when investigating the melting points of the pyrolysis waxes with DSC, a temperature from which the samples start to melt (onset temperature) and a highest peak indicating the point at which the samples have melted completely were recorded. The onset and peak melting temperatures are recorded in Table 3, taken from the endothermic peak identified for the melting of the wax on the DSC thermograms. The melting point values obtained for the HDPE pyrolysis waxes can be compared to commercial paraffin (50-70 °C), microcrystalline (60-91 °C), barnsdall (70-74 °C) and beeswax (63-70 °C) waxes, as observed by Arabiourrutia et al. (2012) when characterising waxes produced from the pyrolysis of polyolefins in a conical spouted bed reactor. The same trend in influence of the pyrolysis parameters is seen in these results as those for the TGA analysis. The pyrolysis temperature is seen to have a more definitive impact on the thermal properties of the waxes (as with chemical characterisation.) With increasing process temperature, higher peak melting points can be observed. Additionally, the waxes produced using a higher carrier gas flowrate and thus lower vapour residence time, also have slightly higher melting points than those

491 produced with the lower nitrogen flowrate. In Section 3.2 it was discussed that the rise of
 492 process temperature results in an increase gasoline range (<C₁₃) compounds, therefore,
 493 containing more lower melting point compounds. The higher melting points seen in the
 494 waxes produced at the higher pyrolysis temperatures (500 and 550 °C) may be explained in
 495 Section 3.3, in which further GC-MS and FTIR analysis of the waxes at different stages of
 496 thermal (and oxidative) ageing are investigated. The waxes produced at higher temperatures
 497 are more olefinic in nature, containing more unsaturated compounds as a result of the
 498 influence of process temperature on the radical mechanisms involved in pyrolysis. Not only
 499 do alkenes have slightly higher melting points than alkanes due to stronger intermolecular
 500 forces, but they are also more prone to oxidation reactions, as indicated by the number of
 501 compounds containing hydroxyl and carbonyl functional groups in Table 4, even at the
 502 unconditioned stage. The hydroxyl and carbonyl groups present within alcohol molecules
 503 require a greater energy to overcome the stronger intermolecular forces of hydrogen bonding,
 504 therefore the melting point of alcohols is higher than that of alkanes with the same chain
 505 length (Purohit and Pradhan, 2013). Additionally, when further exposed to elevated
 506 temperatures in analysis, the more unsaturated waxes may take part in polymerization
 507 reactions to form heavier molecules.

508

509 **Table 3:** Onset and peak melting points of the pyrolysis waxes using DSC.

Sample	Onset (°C)	Peak (°C)
450-2	46.84	49.26
500-2	85.25	88.92
550-2	71.22	78.25
450-4	48.02	49.75
500-4	82.21	86.42
550-4	74.18	87.67

510

511 *3.3 Thermal Ageing of Waxes*

512

513 In this study, it has been established that the pyrolysis operating temperature is the dominant
 514 parameter that influences the chemical and thermal properties of the wax products in the
 515 thermal pyrolysis of HDPE. To further support the thermal characterisation results within this
 516 section and to assess the suitability of the waxes for applications that may involve their
 517 incorporation at temperatures above their melting points, such as in asphalt road construction,
 518 three of the waxes (450-2, 500-2 and 550-2) were selected for thermal conditioning/ageing
 519 and analysis. A further detailed analysis of GC-MS chromatograms was conducted at each

520 stage of the thermal conditioning, including further representative categories for the different
 521 molecular weight components within the waxes; diesel (C₄-C₉), gasoline (C₁₀-C₁₉) and wax
 522 (C₂₀₊) fractions, as seen in Table 4. A focus on compounds that are present in trace-small
 523 amounts and therefore overlooked in the initial analysis by the peak width integration and
 524 identification are also examined to identify possible oxidation products. FTIR analysis was
 525 additionally utilised to examine the change in functional groups present at each stage.

526

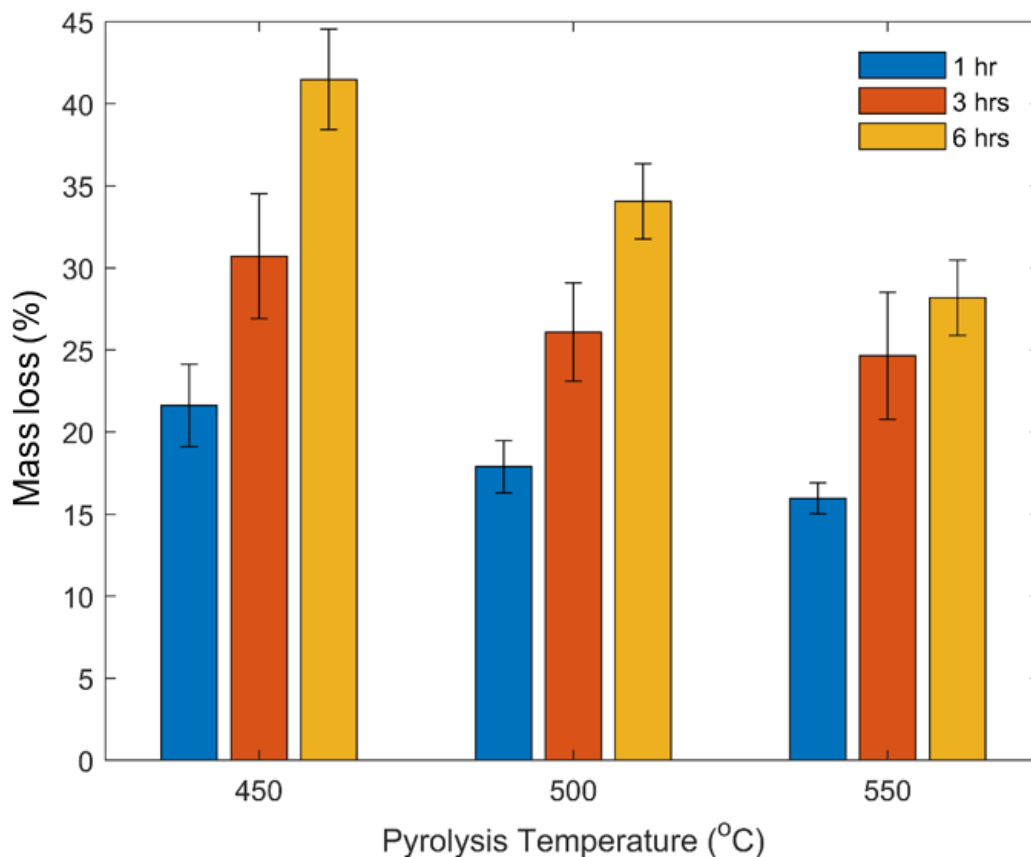
527 **Table 4:** Distribution in weight percentage of molecular weight and class of hydrocarbons in
 528 pyrolysis waxes (450-2, 500-2 and 550-2) after thermal conditioning at 170 °C from 0-6
 529 hours.

Ageing time (hour)	450-2				500-2				550-2			
	0	1	3	6	0	1	3	6	0	1	3	6
Diesel (C ₄ -C ₉)	7.19	3.41	6.30	6.19	7.87	3.54	7.56	10.96	10.42	3.18	7.99	15.57
Gasoline (C ₁₀ -C ₁₉)	62.0	44.89	20.31	1.76	56.89	37.11	10.46	1.15	54.38	31.92	10.54	0
Wax (C ₂₀₊)	30.81	51.70	73.39	92.04	35.24	59.36	81.98	87.89	35.20	64.90	80.92	84.43
Paraffinic	55.76	59.60	58.95	72.46	34.65	41.35	46.29	61.69	35.89	37.84	42.04	49.49
Olefinic	35.92	31.34	29.35	17.41	48.31	45.73	38.90	23.01	50.24	47.12	40.83	28.68
Diene	2.96	2.64	1.55	0.25	7.09	6.79	4.27	0	8.80	8.68	5.96	0
Aromatics	3.27	3.57	6.30	6.19	3.39	3.78	8.71	12.86	2.85	3.18	7.99	18.48
Alcohols	2.08	2.30	3.09	2.61	2.52	2.08	1.59	2.45	2.10	2.43	2.83	2.46
Carbonyls	0	1.39	0.75	1.07	0.16	0.27	0.24	0	0.13	0.74	0.36	0.89

530

531 Due to the wax fractions being cooled swiftly from hot vapors to a low temperature (5 °C)
 532 after leaving the pyrolysis reactor vessel, they contain lightweight components (<C₁₀) that
 533 have boiling points lower than the chosen condition temperature of 170 °C. Significant mass
 534 losses from 15.96-21.61% at 1 hour to 28.2-41.49% at 6 hours were observed (Figure 6) as a
 535 result of the loss of volatiles. A high mass loss indicates high emissions and therefore detailed
 536 information on the low molecular weight hydrocarbons should be evaluated with respect to
 537 influence on the environment and exposure. If the effects are substantial, further efforts to
 538 reduce this should be considered for potential applications. At all time periods, the mass loss
 539 surpasses the initial percentage of compounds with a boiling point below 170 °C, indicating
 540 thermal decomposition taking place of the decreasing gasoline range (C₁₀-C₁₉) to lower
 541 molecular weight components (C₄-C₉), which are emitted by the samples. In all waxes, an
 542 initial significant decrease in diesel (C₄-C₉) fractions is observed within the first hour as the
 543 low boiling point components are emitted and lost from the samples. The fractional category
 544 is then seen characteristically to increase, assumed to be a result of the gasoline (C₁₀-C₁₉)
 545 fractions beginning to thermally decompose upon extended thermal exposure. The diesel

546 fractions again begin to incrementally decrease at 6 hours as the produced lower molecular
547 weight products of thermal decomposition begin to be emitted and lost from the samples.



548 **Figure 6.** Mass loss of pyrolysis waxes with thermal conditioning.
549

550 The heavier wax fraction (C_{20+}) is seen to significantly increase, obviously due to the mass %
551 decrease of the diesel and gasoline fractions. However, the increase in wax components is
552 larger than the overall reductions in the other fractional categories and the total mass loss in
553 the wax samples at the end of the thermal conditioning. Thermal hydrocarbon chemistry
554 involves the degradation of large molecules into smaller ones, but it can also involve the
555 production of heavier molecules (Savage, 2000). The thermal polymerisation of alkenes
556 within the wax may be a contributing reaction to the substantial increase in heavier molecular
557 weight fractions. A reaction such as this can be evident by the sizable drop in percentage of
558 unsaturated (alkene and diene) compounds present in the waxes from the non-conditioned
559 state to 6 hours of thermal conditioning, and the subsequent increase in mass percentage of
560 larger paraffinic hydrocarbons. The peaks in the GC-MS chromatograms were seen to shift to
561 the right, as seen in S3 (a-j.) Additionally, the bands corresponding to olefinic bonds in the
562 FTIR spectra ($890, 900-980, 995, 1645$ and 3040 cm^{-1}) are all seen to decrease or disappear
563 entirely from the spectra throughout the stages of thermal exposure. In the case of not all

564 unsaturated bonds being located at the terminal position of the hydrocarbon chains, this could
565 contribute to the reduction in the two bands at 2960 and 2900 cm^{-1} that correspond to $-\text{CH}_3$
566 terminal groups. The C-H bond stretching of $-\text{CH}_2-$ groups at 725, 2850 and 2920 cm^{-1} are
567 seen to be slightly more elongated in shape but are not significantly changed.

568

569 In the case of self-initiated polymerization, the initiating radicals and mechanisms by which
570 they are formed can be unclear. However, it is noted that the primary and secondary products
571 of paraffin and alkene oxidation, as will be discussed, include hydroperoxides and acids.

572 Hydroperoxide groups are largely used as initiators in radical polymerization reactions with
573 alkenes as these functional groups can break easily, generating free radicals. Acidic reagents
574 are also typically used in cationic polymerization by donating a proton to an alkene to yield
575 long-chain carbocations (Moldoveanu, 2019; Liu, 2021). In the unconditioned waxes, small
576 amounts (2.08-2.52 %) of primary alcohols were detected. This may be attributed to
577 oxidation processes during the cooling of the waxes within the glassware in the instance of
578 oxygen entering the system and upon wax storage prior to analysis. It can be observed in
579 Table 5 that when subjected to heat in oxygen for prolonged times, the number of primary
580 alcohols ($\text{C}_{10}<$) as well as diols are increased, which is supported by the FTIR spectra in S2
581 (a-i.) With increased time of thermal conditioning, the band at 1076 cm^{-1} for primary alcohols
582 significantly increases, while the bands at 2960 and 2900 cm^{-1} for $-\text{CH}_3$ terminal bond groups
583 are decreased. Some cycloalkanes with alcohol substituents such as methanol were also
584 identified, such as Cyclododecanemethanol ($\text{C}_{13}\text{H}_{26}\text{O}$.) Additionally, trace amounts of
585 compounds containing carbonyl functional groups were detected, increasing with
586 conditioning time from the initial unconditioned waxes and including larger chain esters and
587 acids especially. Products such as this are common in the thermal oxidation of paraffin wax
588 conducted at 110-140 $^{\circ}\text{C}$, however, typically with an appropriate catalyst present. This is
589 reported to lead predominantly to the formation of alcohol isomers with the same number of
590 carbon atoms as the initial hydrocarbon molecules, as well as other secondary products
591 including acids, esters, and ketones (Purohit and Pradhan, 2013). The oxidation products
592 identified may also be a result of the oxidation of alkene molecules within the pyrolysis
593 waxes. Alkenes are more susceptible to reactions with oxygen, with the addition of O_2
594 molecules most commonly occurring to the carbon atom adjacent to the double bond (Liu,
595 2021). This produces unstable hydroperoxide molecules that decompose to form two
596 aldehyde or carboxylic acid groups (Liu 2021). This can be observed in the FTIR spectra as
597 the reduced CH_3 band, as previously discussed, and the growing band at 1650-1800 cm^{-1} with

598 conditioning time that corresponds to conjugated and aliphatic aldehydes, carboxylic acids,
599 esters, and ketones.

600

601 **4. Potential of Pyrolysis Wax in Bitumen Modification**

602

603 Asphalt pavement is the most common paving material for highways and urban roads, being
604 a complex mixture comprising of aggregates, filler, bitumen binder, and air voids.

605 Conventional bitumen binders are a by-product of the petroleum refining process with
606 petroleum being a finite and highly impacting resource. A main effort within pavement
607 engineering currently is to move towards “greener” alternatives, aiming to align with
608 sustainable development and circular economy goals (Su et al. 2018; Gaudenzi et al. 2021).

609 Pyrolysis has commonly been used by authors in literature to thermochemically treat waste
610 materials such as biomasses, cooking oils and crumb rubber and study their derived products
611 for the partial replacement and modification of hot mix asphalt (HMA) binders (Kolokolova,
612 2013; Dong et al. 2019). As discussed in previous work by the authors, through concepts such
613 as Design from Recycling, pyrolysis could also be readily applied in the upgrading of waste
614 plastics for such applications (Abdy et al. 2022). Furthermore, the addition of waxes as
615 viscosity and workability improvers in asphalt binders has caught recent interest, with the aim
616 to reduce mixing and compaction temperatures, thus reducing energy consumption, cost, and
617 emission intensity (Edwards, 2008). PE waxes have especially been observed to offer higher
618 softening points, improved chemical stability, distribution, fluidity and water resistance
619 (Prajapati et al. 2021). Authors have noted in particular that the addition of thermally
620 degraded PO polymers such as polypropylene and low-density polyethylene results in an
621 enhanced resistance to permanent deformation, as well as an increase in binder stiffness,
622 temperature resistance, Marshall stability and stripping resistance (Al-Hadidy and Tan,
623 2009a, 2009c). Further exploration into this area of research that can provide detailed and
624 optimisable pyrolysis processes and in-depth product characterisation for this application is
625 still needed.

626

627 **5. Conclusions**

628

629 The findings in this paper show that the fixed-bed reactor vessel produced for this study was
630 efficient for the thermal pyrolysis of HDPE at moderate temperatures (450-550 °C), which
631 allowed for obtaining (in batch mode) a yield of up to 91.87% wax at 500 °C. The waxes

632 produced at higher temperatures were mainly olefinic, due to higher temperatures promoting
633 certain thermal degradation radical mechanisms, such as β -scission. The melting points of the
634 waxes were within the range of 49-89 °C, corresponding to commercial waxes that are
635 typically used as flow improvers and performance enhancers in hot-mix asphalt, or as low
636 temperature additives in warm-mix asphalt.

637

638 Relationships between the process operating parameters and resultant waxes were
639 established, with a novel focus on the thermal properties and ageing performance of the
640 waxes, especially with regards to volatile loss and ageing mechanisms that occur. The more
641 olefinic waxes produced at higher temperatures and higher nitrogen flowrates (having the
642 lowest vapour residence times) saw the lowest volatile mass loss. They were observed to be
643 more prone to oxidation and polymerization reactions, the products from each supporting the
644 higher melting point and thermal stability of these waxes. The lowest loss in volatiles was
645 seen for the wax produced at 550 °C, inferring that it would be the optimal wax to blend with
646 asphalt binders. For HMA modification purposes, blending at temperatures lower than 170
647 °C should be considered to lessen the volatile loss with initial blending and storage of the
648 wax modified binders. In the case of significant volatile loss, further efforts to reduce this
649 should be considered for potential applications. The relationship between pyrolysis
650 parameters, resultant wax properties and their subsequent performance and compatibility as
651 binder modifiers in hot-mix asphalt is not yet fully realised and will be investigated in
652 following papers.

653

654 **6. Supplementary Materials**

655

656 **Figure S1:** GC-MS chromatograms for (a) 450-2 (450 °C, 2 L/min N₂ flowrate) wax, (b)
657 500-2 (500 °C, 2 L/min N₂ flowrate) wax, (c) 550-2 (550 °C, 2 L/min N₂ flowrate) wax, (d)
658 chromatogram depicting homologous series of triplets which is indicative of PE
659 depolymerisation, (e) 450-4 (450 °C, 4 L/min N₂ flowrate) wax, (f) 500-4 (500 °C, 4 L/min
660 N₂ flowrate) wax, (g) 550-4 (550 °C, 4 L/min N₂ flowrate) wax. **Figure S2:** FTIR spectrum
661 for (a) 450-2 wax, 1 hour @ 170°C, (b) 500-2 wax, 1 hour @ 170 °C, (c) 550-2 wax, 1 hour
662 @ 170 °C, (d) 450-2 wax, 3 hours @ 170 °C, (e) 500-2 wax, 3 hours @ 170 °C, (f) 550-2
663 wax, 3 hours @ 170 °C, (g) 450-2 wax, 6 hours @ 170 °C, (h) 500-2 wax, 6 hours @ 170 °C,
664 (i) 550-2 wax, 6 hours @ 170 °C. **Figure S3:** GC-MS chromatograms for (a) 450-2 wax, 1
665 hour @ 170 °C, (b) 500-2 wax, 1 hour @ 170 °C, (c) 550-2 wax, 1 hour @ 170 °C, (d)

666 Chromatogram depicting the alcohol and carbonyl containing compounds between triplets as
667 a result of oxidation reactions, (e) 450-2 wax, 3 hours @ 170 °C, (f) 500-2 wax, 3 hours @
668 170 °C, (g) 550-2 wax, 3 hours @ 170 °C, (h) 450-2 wax, 6 hours @ 170 °C, (i) 500-2 wax, 6
669 hours @ 170 °C, (j) 550-2 wax, 6 hours @ 170 °C.

670

671 **7. Acknowledgements**

672

673 The authors would like to acknowledge the financial support of a PhD studentship provided
674 by Aggregate Industries UK Ltd. and Aston University. The author Jiawei Wang would also
675 like to acknowledge the support from Guangdong Science and Technology Program, No.
676 2021A0505030008.

677

678 **8. Declaration of Competing Interest**

679

680 The authors declare that they have no known competing financial interests or personal
681 relationships that could have appeared to influence the work reported in this paper.

682

683 **9. References**

684

685 Abdy, C., Zhang, Y., Wang, J., Yang, Y., Artamendi, I., Allen, B., 2022. Pyrolysis of
686 polyolefin plastic waste and potential applications in asphalt road construction: A technical
687 review. *Resour. Conserv. Recycl.* 180, 106213.
688 <https://doi.org/10.1016/j.resconrec.2022.106213>

689

690 Adrados, A., de Marco, I., Caballero, B.M., López, A., Laresgoiti M.F., Torres A., 2012.
691 Pyrolysis of plastic packaging waste: A comparison of plastic residuals from material
692 recovery facilities with simulated plastic waste. *Waste Manag.* 32 (5), 826-832.
693 <https://doi.org/10.1016/j.wasman.2011.06.016>.

694

695 Aguado, R., Olazar, M., San José, M.J., Gaisán, B., Bilbao, J., 2002. Wax formation in the
696 pyrolysis of polyolefins in a conical spouted bed reactor. *Energy Fuel.* 16 (6), 1429-1437.
697 <https://doi.org/10.1021/ef020043w>.

698

699 Al-Hadidy, A.I., Tan Y. Q., 2009a. Evaluation of Pyrolysis LDPE Modified Asphalt Paving
700 Materials. *J. Mater. Civ. Eng.* 21 (10), 618-623. [https://doi.org/10.1061/\(ASCE\)0899-
701 1561\(2009\)21:10\(618\)](https://doi.org/10.1061/(ASCE)0899-1561(2009)21:10(618)).

702

703 Al-Hadidy, A.I., Tan Y. Q., 2009b. Effect of polyethylene on life of flexible pavements.
704 *Constr. Build. Mater.* 23 (3), 1456-1464. <https://doi.org/10.1016/j.conbuildmat.2008.07.004>.

705

706 Al-Hadidy, A.I., Tan Y. Q., 2009c. Mechanistic approach for polypropylene-modified
707 flexible pavements. *Mater. Des.* 30 (4), 1133-1140.
708 <https://doi.org/10.1016/j.matdes.2008.06.021>.
709

710 Al-Salem, S. M., Lettieri, P., Baeyens, J., 2009. Recycling and recovery routes of plastic
711 solid waste (PSW): A review. *Waste Manag.* 29 (10), 2625-2643.
712 <https://doi.org/10.1016/j.wasman.2009.06.004>.
713

714 Al-Salem, S. M., Antelava, A., Constantinou, A., Manos, G., Dutta, A., 2017. A review on
715 thermal and catalytic pyrolysis of plastic solid waste (PSW). *J. Environ. Manag.* 197: 177-
716 198. <https://doi.org/10.1016/j.jenvman.2017.03.084>.
717

718 Al-Salem, S. M., 2019. Thermal pyrolysis of high density polyethylene (HDPE) in a novel
719 fixed bed reactor system for the production of high value gasoline range hydrocarbons (HC).
720 *Process Saf. Environ.* 127, 171-179. <https://doi.org/10.1016/j.psep.2019.05.008>.
721

722 Al-Salem, S.M., Yang, Y., Wang, J., Leeke, G. A., 2020. Pyro-Oil and Wax Recovery from
723 Reclaimed Plastic Waste in a Continuous Auger Pyrolysis Reactor. *Energies.* 13 (8), 2040.
724 <https://doi.org/10.3390/en13082040>.
725

726 Al-Salem, S.M., Dutta, A., 2021. Wax Recovery from the Pyrolysis of Virgin and Waste
727 Plastics. *Ind. Eng. Chem. Res.* 60 (22), 8301-8309. <https://doi.org/10.1021/acs.iecr.1c01176>.
728

729 Arabiourrutia, M., Elordi, G., Lopez, G., Borsella, E., Bilbao, J., Olazar, M., 2012.
730 Characterization of the waxes obtained by the pyrolysis of polyolefin plastics in a conical
731 spouted bed reactor. *J. Anal. Appl. Pyrolysis.* 94, 230-237.
732 <https://doi.org/10.1016/j.jaap.2011.12.012>.
733

734 Bockhorn, H., Hornung, A., Hornung, U., Schawaller, D., 1999. Kinetic study on the thermal
735 degradation of polypropylene and polyethylene. *J. Anal. Appl. Pyrolysis.* 48 (2), 93-109.
736 [https://doi.org/10.1016/S0165-2370\(98\)00131-4](https://doi.org/10.1016/S0165-2370(98)00131-4).
737

738 BSOL British Standards Online, 2012. BS EN 14769 Bitumen and bituminous binders.
739 Accelerated long-term ageing conditioning by a Pressure Ageing Vessel (PAV).
740 <https://bsol.bsigroup.com/> (accessed 1 January 2022).
741

742 BSOL British Standards Online, 2014. BS EN 12607 Bitumen and bituminous binders.
743 Determination of the resistance to hardening under influence of heat and air. RTFOT method.
744 <https://bsol.bsigroup.com/> (accessed 1 January 2022).
745

746 Chaala, A., Darmstadt, H., Roy, C., 1997. Vacuum pyrolysis of electric cable wastes. *J. Anal.*
747 *Appl. Pyrolysis.* 39 (1), 79-96. [https://doi.org/10.1016/S0165-2370\(96\)00964-3](https://doi.org/10.1016/S0165-2370(96)00964-3).
748

749 Desidery, L., Lanotte, M., 2021. Effect of Waste Polyethylene and Wax-Based Additives on
750 Bitumen Performance. *Polymers.* 13 (21), 3733. <https://doi.org/10.3390/polym13213733>.
751

752 Dharmaraj, S., Ashokkumar, V., Pandiyan, R., Halimatul Munawaroh, H.S., Chew, K.W.,
753 Chen, W.H., Ngamcharussrivichai, C., 2021. Pyrolysis: An effective technique for
754 degradation of COVID-19 medical wastes. *Chemosphere* 275, 130092-130092.
755 <https://doi.org/10.1016/j.chemosphere.2021.130092>

756
757 Dimondo, D., Guillon, C., 2017. Polymer-modified asphalt with wax additive.
758 <https://patents.google.com/patent/WO2017136957A1/en/> (accessed 19 August 2022).
759
760 Dong, R., Zhao, M., Tang, N., 2019. Characterization of crumb tire rubber lightly pyrolyzed
761 in waste cooking oil and the properties of its modified bitumen. *Constr. Build. Mater.* 195,
762 10-18. <https://doi.org/10.1016/j.conbuildmat.2018.11.044>
763
764 Dwivedi, A., 2017. Studies In Properties Of Different Waxes Using DSC And Correlating
765 These With The Properties Obtained by Conventional Methods. Proceedings of the
766 CHEMCON conference, Haldia West Bengal, September 2018. *Int. J. Res. Sci. Eng.*
767 CHEMCON Special Issue, March 2018, 192-197.
768
769 Edwards, Y., 2008. Influence of waxes on polymer modified mastic asphalt performance.
770 Proceedings of the Eurasphalt & Eurobitume Congress, Copenhagen, 21-23 May 2008. Paper
771 No. 401-014.
772
773 Fazaeli, H., Behbahani, H., Amini, A.A., Rahmani, J., Yadollahi, G., 2012. High and Low
774 Temperature Properties of FT-Paraffin-Modified Bitumen. *Adv. Mater. Sci. Eng.* 2012,
775 406791. <https://doi.org/10.1155/2012/406791>.
776
777 Gaudenzi, E., Canestrari, F., Lu, X., 2021. Performance Assessment of Asphalt Mixture
778 Produced with a Bio-Based Binder. *Materials.* 14 (4), 918.
779 <https://doi.org/10.3390/ma14040918>.
780
781 Ghasr, S.F., Abedini, H., 2017. Predicting the distribution of thermal pyrolysis of high
782 density polyethylene products using a mechanistic model. *Model. Earth. Syst. Environ.* 3 (1),
783 40. <https://doi.org/10.1007/s40808-017-0309-9>.
784
785 Grady, B. P., 2021. Waste plastics in asphalt concrete: A review. *SPE Polymers.* 2 (1), 4-18.
786 <https://doi.org/10.1002/pls2.10034>.
787
788 Hernández, M.D.R., Gómez, A., García, A.N., Agulló, J. J., Marcilla, A., 2007. Effect of the
789 temperature in the nature and extension of the primary and secondary reactions in the thermal
790 and HZSM-5 catalytic pyrolysis of HDPE. *Appl. Catal. A.* 317 (2), 183-194.
791 <https://doi.org/10.1016/j.apcata.2006.10.017>.
792
793 Hilten, R. N., Das, K. C., 2010. Comparison of three accelerated aging procedures to assess
794 bio-oil stability. *Fuel.* 89 (10), 2741-2749. <https://doi.org/10.1016/j.fuel.2010.03.033>.
795
796 Horvat, N., 1999. Tertiary polymer recycling: study of polyethylene thermolysis as a first
797 step to synthetic diesel fuel. *Fuel.* 78, 459-470. [https://doi.org/10.1016/S0016-](https://doi.org/10.1016/S0016-2361(98)00158-6)
798 [2361\(98\)00158-6](https://doi.org/10.1016/S0016-2361(98)00158-6).
799
800 Jambeck, J. R., Geyer, R., Wilcox, C., Siegler, T. R., Perryman, M., Andrady, A., Narayan,
801 R., Law, K. L., 2015. Plastic waste inputs from land into the ocean. *Science.* 347 (6223), 768-
802 771. <https://doi.org/10.1126/science.1260352>.
803
804 Jung, S.H., Cho, M.H., Kang, B.S., Kim, J. S., 2010. Pyrolysis of a fraction of waste
805 polypropylene and polyethylene for the recovery of BTX aromatics using a fluidized bed

806 reactor. *Fuel. Process. Technol.* 91 (3), 277-284.
807 <https://doi.org/10.1016/j.fuproc.2009.10.009>.
808
809 Kim, Y., Lim, J., Lee, M., Kown, S., Hwang, S., Wei, L., 2013. Comprehensive Evaluation of
810 Polymer-Modified SMA Mixture Produced with New Polyethylene Wax-Based WMA
811 Additive with Adhesion Promoter. Proceedings of the Transportation Research Board 92nd
812 Annual Meeting, Washington DC, United States, 13-17 January 2013.
813
814 Kolokolova, O., 2013. Biomass Pyrolysis and Optimisation for Bio-bitumen. Doctoral
815 Thesis, University of Canterbury.
816
817 Kumar, S., Singh, R. K., 2011. Recovery of hydrocarbon liquid from waste high density
818 polyethylene by thermal pyrolysis. *Braz. J. Chem. Eng.* 28 (4), 659-667.
819 <https://doi.org/10.1590/S0104-66322011000400011>.
820
821 Kumar, S., Singh, R. K., 2013. Thermolysis of High-Density Polyethylene to Petroleum
822 Products. *J. Petrol. Eng.* 2013 (6), 987568. <https://doi.org/10.1155/2013/987568>.
823
824 Leng, Z., Padhan, R. K., Sreeram, A., 2018. Production of a sustainable paving material
825 through chemical recycling of waste PET into crumb rubber modified asphalt. *J. Clean. Prod.*
826 180, 682-688. <https://doi.org/10.1016/j.jclepro.2018.01.171>.
827
828 Ling, T., Lu, Y., Zhang, Z., Li, C., Oeser, M., 2019. Value-added application of waste rubber
829 and waste plastic in asphalt binder as a multifunctional additive. *Materials*. 12 (8), 16-19.
830 <https://doi.org/10.3390/ma12081280>.
831
832 Liu, X., 2021. Organic Chemistry I, Kwantlen Polytechnic University.
833
834 Lund, L.M., Sandercock, P.M.L., Basara, G.J., Austin, C. C., 2008. Investigation of various
835 polymeric materials for set-point temperature calibration in pyrolysis-gas chromatography-
836 mass spectrometry (Py-GC-MS). *J. Anal. Appl. Pyrolysis*. 82 (1), 129-133.
837 <https://doi.org/10.1016/j.jaap.2008.02.002>.
838
839 Mastral, F. J., Esperanza, E., Berruenco, C., Juste, M., Ceamanos, J., 2003. Fluidized bed
840 thermal degradation products of HDPE in an inert atmosphere and in air-nitrogen mixtures.
841 *J. Anal. Appl. Pyrolysis*. 70 (1), 1-17. [https://doi.org/10.1016/S0165-2370\(02\)00068-2](https://doi.org/10.1016/S0165-2370(02)00068-2).
842
843 Mastral, J. F., Berruenco, C., Ceamanos, J., 2007. Theoretical prediction of product
844 distribution of the pyrolysis of high density polyethylene. *J. Anal. Appl. Pyrolysis*. 80 (2),
845 427-438. <https://doi.org/10.1016/j.jaap.2006.07.009>.
846
847 Miandad, R., Rehan, M., Barakat, M., Aburizaiza, A., Khan, H., Ismail, I., Dhavamani, J.,
848 Gardy, J., Hassanpour, A., Nizami, A. S., 2019. Catalytic pyrolysis of plastic waste: Moving
849 toward pyrolysis based biorefineries. *Front. Energy Res.* 7, 1-27.
850 <https://doi.org/10.3389/fenrg.2019.00027>.
851
852 Moldoveanu, S. C., 2019. Pyrolysis of Organic Molecules, second ed. Chapter 6 - Pyrolysis
853 of Peroxy Compounds, 311-319.
854

855 Nakhaei, M., Darbandi Olia, A.D., Akbari Nasrekani, A., Asadi, P., 2016. Rutting and
856 moisture resistance evaluation of polyethylene wax–modified asphalt mixtures. *Pet. Sci.*
857 *Technol.* 34 (17-18), 1568-1573. <https://doi.org/10.1080/10916466.2016.1212209>.
858

859 Onwudili, J. A., Insura, N., Williams, P. T., 2009. Composition of products from the
860 pyrolysis of polyethylene and polystyrene in a closed batch reactor: Effects of temperature
861 and residence time. *J. Anal. Appl. Pyrolysis.* 86 (2), 293-303.
862 <https://doi.org/10.1016/j.jaap.2009.07.008>.
863

864 Park, J.J., Park, K., Park, J.W., Kim, D. C., 2002. Characteristics of LDPE pyrolysis. *Korean*
865 *J. Chem. Eng.* 19 (4), 658-662. <https://doi.org/10.1007/BF02699313>.
866

867 Prajapati, R., Kohli, K., Maity S.K., Sharma, B. K., 2021. Potential Chemicals from Plastic
868 Wastes. *Molecules.* 26 (11), 3175. <https://doi.org/10.3390/molecules26113175>.
869

870 Purohit S.J., Pradhan, M., 2013. Paraffin Oxidation Studies. *Int. J. Eng. Innov. Res.* 2 (1), 75.
871 <https://ijeir.org/> (accessed 19 August 2022).
872

873 Quesada, L., Hoces, M.C.D., Martín-Lara, M. A., Luzón, G., Blázquez, G., 2020.
874 Performance of Different Catalysts for the In Situ Cracking of the Oil-Waxes Obtained by the
875 Pyrolysis of Polyethylene Film Waste. *Sustainability.* 12 (13) 1-15.
876 <https://doi.org/10.3390/su12135482>.
877

878 Ragaert, K., Delva, L., Van Geem, K., 2017. Mechanical and chemical recycling of solid
879 plastic waste. *Waste Manag.* 69, 24-58. <https://doi.org/10.1016/j.wasman.2017.07.044>.
880

881 SASOL, 2018. Sasobit REDUX Product information. <https://www.sasobit.com/en/redux/>
882 (accessed 31 May 2022).
883

884 Savage, P. E. (2000). Mechanisms and kinetics models for hydrocarbon pyrolysis. *J. Anal.*
885 *Appl. Pyrolysis.* 54 (1), 109-126. [https://doi.org/10.1016/S0165-2370\(99\)00084-4](https://doi.org/10.1016/S0165-2370(99)00084-4).
886

887 Seeger, M., Barrall, E. M., 1975. Pyrolysis–gas chromatographic analysis of chain branching
888 in polyethylene. *J. Polym. Sci.* 13 (7), 1515-1529.
889 <https://doi.org/10.1002/pol.1975.170130704>.
890

891 Shang, L., Wang, S., 2011. Pyrolysed Wax from Recycled Crosslinked Polyethylene as a
892 Warm-Mix Asphalt (WMA) Additive for Crumb-Rubber-Modified Asphalt. *Prog. Rubber*
893 *Plast. Recycl. Technol.* 27 (3), 133-144. <https://doi.org/10.1177/147776061102700301>.
894

895 Su, N., Xiao, F., Wang, J., Cong, L., Amirkhani, S., 2018. Productions and applications of
896 bio-asphalts – A review. *Constr. Build. Mater.* 183, 578-591.
897 <https://doi.org/10.1016/j.conbuildmat.2018.06.118>.
898

899 Sukhija, M., Saboo, N., 2021. A comprehensive review of warm mix asphalt mixtures-
900 laboratory to field. *Constr. Build. Mater.* 274, 121781-121781.
901 <https://doi.org/10.1016/j.conbuildmat.2020.121781>.
902

903 Szulejko, J., Kim, Y.H., Kim, K. H., 2013. Method to predict gas chromatographic response
904 factors for the trace-level analysis of volatile organic compounds based on the effective

905 carbon number concept. *J. Separ. Sci.* 36, 3356-3365.
906 <https://doi.org/10.1002/jssc.201300543>.
907
908 Tsai, C. J., Chen, M. L., Chang, K. F., Chang, F. K., Mao, I. F., 2009. The pollution
909 characteristics of odor, volatile organochlorinated compounds and polycyclic aromatic
910 hydrocarbons emitted from plastic waste recycling plants. *Chemosphere*. 74 (8), 1104-1110.
911 <https://doi.org/10.1016/j.chemosphere.2008.10.041>.
912
913 Verma, R., Vinoda, K. S., Papireddy, M., Gowda, A.N.S., 2016. Toxic Pollutants from
914 Plastic Waste- A Review. *Proc. Environ. Sci.* 35, 701-708.
915 <https://doi.org/10.1016/j.proenv.2016.07.06>.
916
917 Westerhout, R.W.J., Kuipers, J., Swaaij, V., 1998. Experimental Determination of the Yield
918 of Pyrolysis Products of Polyethene and Polypropene. *Ind. Eng. Chem. Res.* 37 (3), 841-847.
919 <https://doi.org/10.1021/ie970384a>.
920
921 Williams, P.T., Williams, E. A., 1997. The pyrolysis of individual plastics and a plastic
922 mixture in a fixed bed reactor. *J. Chem. Technol. Biotechnol.* 70 (1), 9-20.
923 [https://doi.org/10.1002/\(SICI\)1097-4660\(199709\)70:1<9::AID-JCTB700>3.0.CO;2-E](https://doi.org/10.1002/(SICI)1097-4660(199709)70:1<9::AID-JCTB700>3.0.CO;2-E).
924
925 Williams, P.T., Williams, E. A., 1999a. Fluidised bed pyrolysis of low density polyethylene
926 to produce petrochemical feedstock. *J. Anal. Appl. Pyrolysis.* 51 (1-2), 107-126.
927 [https://doi.org/10.1016/S0165-2370\(99\)00011-X](https://doi.org/10.1016/S0165-2370(99)00011-X).
928
929 Williams, P.T., Williams, E. A., 1999b. Interaction of Plastics in Mixed-Plastics Pyrolysis.
930 *Energy. Fuels.* 13 (1), 188-196. <https://doi.org/10.1021/ef980163x>.
931
932 Yang, X., You, Z., Mills-Beale, J., 2015. Asphalt Binders Blended with a High Percentage of
933 Biobinders: Aging Mechanism Using FTIR and Rheology. *J. Mater. Civ. Eng.* 27 (4),
934 04014157. [https://doi.org/10.1061/\(ASCE\)MT.1943-5533.0001117](https://doi.org/10.1061/(ASCE)MT.1943-5533.0001117).
935
936 Yu, H., Leng, Z., Gao, Z., 2016. Thermal analysis on the component interaction of asphalt
937 binders modified with crumb rubber and warm mix additives. *Constr. Build. Mater.* 125, 168-
938 174. <https://doi.org/10.1016/j.conbuildmat.2016.08.032>.
939
940 Zaumanis M., Haritonovs, V., 2010. Research on properties of warm mix asphalt. *Sci J Riga*
941 *Tech Univ Constr Sci.* 11, 77-84. <https://ortus.rtu.lv/science/en/publications/9776/fulltext/>
942 (accessed 14 November 2022).
943